

# X-ray Observations of Mrk 231

T.J.Turner<sup>1,2,3</sup>

## ABSTRACT

This paper presents new X-ray observations of Mrk 231, an active galaxy of particular interest due to its large infrared luminosity and the presence of several blueshifted broad absorption line (BAL) systems, a phenomenon observed in a small fraction of QSOs.

A *ROSAT* HRI image of Mrk 231 is presented, this shows an extended region of soft X-ray emission, covering several tens of kpc, consistent with the extent of the host galaxy. An *ASCA* observation of Mrk 231 is also presented. Hard X-rays are detected but the data show no significant variability in X-ray flux. The hard X-ray continuum is heavily attenuated and X-ray column estimates range from  $\sim 2 \times 10^{22} - 10^{23} \text{cm}^{-2}$  depending on whether the material is assumed to be neutral or ionized, and on the model assumed for the extended X-ray component. These *ASCA* data provide only the second hard X-ray spectrum of a BAL AGN presented to date. The broad-band spectral-energy-distribution of the source is discussed. While Mrk 231 is X-ray weak compared to Seyfert 1 galaxies, it has an optical-to-X-ray spectrum typical of a QSO.

*Subject headings:* galaxies:active – galaxies:nuclei – X-rays: galaxies – galaxies: individual (Mrk 231)

## 1. Introduction

Recent observations of luminous infrared galaxies (LIGs) indicate that most occur in interacting systems. It is thought that galaxy interactions can fuel Seyfert-type activity in galactic nuclei (e.g. Xia et al. 1998 and references therein) and also result in prodigious

---

<sup>1</sup>Laboratory for High Energy Astrophysics, Code 660, NASA/Goddard Space Flight Center, Greenbelt, MD 20771

<sup>2</sup>Universities Space Research Association

<sup>3</sup>Present address, University of Maryland, Baltimore County

starburst activity, often observed close to the nucleus. Observations in the infrared (IR) band show strong emission from galaxies dominated by starburst activity. It is often difficult to determine whether these galaxies also have active nuclei, based on the IR data alone. Radio and X-ray observations help clarify the picture. The amount of radio and X-ray emission expected from the observed starburst regions can be predicted, from observation of the phenomenon in normal galaxies (David et al. 1992). Some authors suggest that LIGs represent an early phase of evolution for active galactic nuclei (AGN); Lipari, Terlevich and Macchetto (1993) found that most AGN which have strong FeII emission are also LIGs. Mrk 231 ( $z=0.042$ ) is an ultraluminous infrared galaxy, and one of the strongest known FeII emitters. Furthermore, Mrk 231 has one of the highest bolometric luminosities in the local ( $z < 0.1$ ) universe (Sanders et al. 1988) with  $M_v = -22.5$  (Rieke & Low 1972),  $L_{8-1000\mu m} \sim 4 \times 10^{12} L_\odot$  (Soifer et al. 1986),  $L_{IR}/L_B \sim 200$  (Lipari, Colina & Macchetto 1994) and  $L_{BOL} > 10^{46} \text{erg s}^{-1}$  (Soifer et al. 1987). Boksenberg et al. (1977) show that an active nucleus exists in Mrk 231; broad emission lines are observed from permitted transitions, the species and line widths are similar to those defining the Seyfert 1 class. However, no narrow emission lines are seen except for O[II]  $\lambda 3727$ . This O[II] emission line is probably produced in gas which is ionized by hot young stars (Smith et al. 1995) rather than by ultraviolet radiation from the nucleus, since the latter is unlikely to emerge through the dense circumnuclear absorber. The absence of narrow emission lines is sometimes observed in quasi-stellar objects (QSOs) but not in Seyfert galaxies. Another extraordinary property of Mrk 231 is the high polarization,  $\sim 20\%$  at  $2800 \text{ \AA}$  (e.g. Smith et al. 1995, after accounting for dilution from hot stars). In this case the polarized flux is thought to be nuclear emission scattered from circumnuclear dust (Smith et al. 1995).

Mrk 231 is radio-quiet but Smith, Lonsdale & Lonsdale (1998) find the strength and compactness of the VLBI (milli-arcsecond) radio emission to infer the presence of an active nucleus. Bryant & Scoville (1996) find that starburst activity can only account for 40% of the IR luminosity in Mrk 231, supporting the evidence for an active nucleus, which must power the remaining emission. *HST* data showed a compact nucleus enclosed on the south side by a dense arc of star-forming knots concentrated  $\sim 3 - 4''$  away (Surace et al. 1998).

It has also been suggested that there is a connection between the presence of strong FeII emission and blueshifted absorption systems (Hartig & Baldwin 1986; Weymann et al. 1991; Lawrence et al. 1997), although the physical origin of this connection is unclear. Mrk 231 has several blueshifted Broad Absorption Line (BAL) systems evident in the ultraviolet data. Adams (1972), Boksenberg et al. (1977), Arakelian et al. (1971), Boroson et al. (1991), Rudy et al. (1985) and others discuss three distinguishable absorption systems in Mrk 231. The most prominent is defined by NaI, CaII and HeI lines originating in gas with an outflow velocity  $\sim 4200 \text{ km s}^{-1}$  relative to the line emission seen in the source. A

second system shows only the D lines of NaI and an outflow velocity  $\sim 6000 \text{ km s}^{-1}$ . A third system is observed in Balmer and CaII absorption lines and has a redshift implying inflow at a velocity  $\sim 200 \text{ km s}^{-1}$ . A fourth system appeared between 1984 December and 1988 May, with prominent NaI D and HeI absorption at an outflow velocity of  $\sim 8000 \text{ km s}^{-1}$  (Boroson et al. 1991, Kollatschney, Dietrich & Hagan 1992). Further absorption variability was observed when a NaI D line disappeared between 1991 and 1994 and the profile of some lines varied (Forster et al. 1995).

Rudy et al. (1985) showed that the shapes of absorption features and velocities in the absorbing gas systems of Mrk 231 are the same as those observed in BAL QSOs and the gas is probably accelerated by the same mechanism. Thus Mrk 231 offers an opportunity to study the BAL phenomenon at low redshift, and with a component containing species of unusually low ionization-state. Most BAL systems are dominated by high-ionization species such as C IV  $\lambda\lambda 1548, 1551$ ; Si IV  $\lambda\lambda 1394, 1403$  and N V  $\lambda\lambda 1239, 1243$  and only a small percentage of sources ( $\sim 15\%$ ) show absorption by low-ionization species, such as Mg II  $\lambda\lambda 2796, 2803$ ; Al III  $\lambda 1671$ ; Al III  $\lambda\lambda 1855, 1863$  and C II  $\lambda 1335$  (Voit, Weymann & Korista 1993). Absorption by Na I D, He I  $\lambda 3889$  and Mg I  $\lambda 2853$  as observed in Mrk 231, is quite rare. The detection of a  $10\mu\text{m}$  silicate absorption feature indicates that dust is an important constituent of at least one of the absorbing systems in Mrk 231 (Roche, Aitken & Whitmore 1983). Forster et al. (1995) conclude the absorption systems are most likely associated with Mrk 231, rather than intervening galaxies, although they find no evidence these systems are linked to a starburst-superwind in this case. Rudy et al. (1985) also point out that the axial ratio in this source is 0.48 (minor/major), and so the source is observed too close to a face-on orientation for the BAL gas to be consistent with interstellar clouds in the plane of the host galaxy. Mrk 231 also contains an OH maser (Baan 1985) and a CO emission region to the nucleus (Scoville et al. 1989). Bryant & Scoville (1996) estimate that  $\sim 3.4 \times 10^9 M_{\odot}$  of gas lies within a radius 420 pc of the nucleus and the material is most likely in the form of a disk.

New X-ray observations of Mrk 231 are presented in this paper. In §2 the *ROSAT* HRI image of the source is shown, and the soft X-ray spectrum observed by the PSPC is discussed. In §3 an *ASCA* observation of Mrk 231 is presented, which provides the first hard X-ray observation of this source, and only the second hard X-ray spectrum of a BAL AGN in the literature.

## 2. The ROSAT Observations

Mrk 231 was observed by the *ROSAT* High Resolution Instrument (HRI) between 1996 May 12 and 1996 June 11, with a total exposure time of 31 ks. Fig 1 shows the HRI image, in  $1''$  bins, smoothed with a Gaussian of width  $\sigma = 1.5''$ . A white cross shows the position of the optical and radio nucleus (Surace et al. 1998) and the white bar shows an extent of  $10''$ . Two X-ray peaks are evident, spaced  $\sim 13''$  apart. There is also the suggestion of asymmetric extent, with an extended region of X-ray flux west of the peaks. There are several other bright point sources in the HRI image, and two were identified as the AGN F219\_015 and F219\_045. The optical positions (obtained from NED, which contains a p.comm. from Keith Mason) and the HRI positions for these AGN agreed to within  $\sim 3''$ , indicating an accurate aspect-solution for this image. The optical position of the nucleus is coincident with the region of relatively low X-ray flux, rather than the X-ray peaks in Fig. 1. There are several other serendipitous point sources in the HRI image and none show the X-ray extent evident in Mrk 231 demonstrating that the extended emission observed for Mrk 231 is real and not an artifact of attitude reconstruction problems in the HRI image.

The *HST* image of Mrk 231 shows a great deal of structure (Surace et al. 1998, c.f. their Fig. 7), most notably a region of emission to the NW of the Seyfert nucleus, composed of knots of emission from star formation. Another distinct peak in the *HST* data lies  $\sim 4''$  south of the nucleus, again due to star formation. The extended emission in the X-ray image seems to be similar in shape, but on a size-scale a factor of  $\sim 3$  larger than that of the bright star-forming knots evident in the *HST* image. At a redshift  $z=0.042$ ,  $1''$  corresponds to  $\sim 1$  kpc (assuming  $H_0 = 50 \text{ km s}^{-1} \text{ Mpc}^{-1}$ ,  $q_0 = 0.5$ ) and so the HRI image implies emission across a total diameter of  $\sim 30$  kpc. Comparison with the *HST* image of Surace et al. (1998; their Fig. 1) shows the X-ray emission matches the optical extent of the host galaxy. The total flux was  $F(0.5 - 2 \text{ keV}) = 1 \pm 0.1 \times 10^{-13} \text{ erg cm}^{-2} \text{ s}^{-1}$  (assuming the spectral model derived from the PSPC fit, as noted below). The luminosity in the observed X-ray emission is  $L(0.1 - 2 \text{ keV}) \sim 10^{42} \text{ erg s}^{-1}$  and so is higher than expected from the summed emission of stars and hot gas in a normal galaxy, but may be related to the starburst activity. The nucleus appears relatively weak in the  $0.1 - 2 \text{ keV}$  band, perhaps because it is more heavily absorbed than emission from regions further out in the galaxy.

Light curves were extracted from circular regions of radius  $6''$  centered on each of the X-ray peaks. No significant variability was evident in the time series from either region. The flux of the two peaks is almost equal, in the soft X-ray band. The flux of the NW peak is  $47 \pm 9$  % of the total flux in the pair.

The *ROSAT* PSPC observed Mrk 231 1991 June 7 – 8 for a total of 24 ks. The two peaks evident in the HRI image cannot be resolved using the PSPC data (which

has a point-spread-function of width  $FWHM \sim 25''$ ). The data were corrected for time-dependent effects using the tool PCPICOR v 2.2.0. Source data were extracted from a cell of radius  $1.3'$  and background data from an annular region centered on the source (but excluding some parts of the image contaminated by serendipitous sources). The PSPC spectrum has already been presented by Rigopoulou, Lawrence and Rowan-Robinson (1996). Those authors noted a poor fit to a power-law model, attenuated by a column of neutral material. That result is confirmed here, yielding  $\chi^2 = 42$  for 18 degrees of freedom ( $dof$ ).

The fit is significantly improved (at  $> 99\%$  confidence) by addition of a narrow gaussian line with rest-energy  $E = 0.86 \pm 0.06$  keV and equivalent width  $EW = 490 \pm 190$  eV ( $\chi^2/dof = 20.0/15$ ) confirming the Rigopoulou et al. (1996) result and yielding a flux  $F(0.5 - 2 \text{ keV}) = 1 \times 10^{-13} \text{ erg cm}^{-2} \text{ s}^{-1}$ . This flux is in excellent agreement with that from the same region in the HRI observation, as expected given the extent of the emission. Strong line emission would be expected if the soft X-rays are from a region of starburst emission, and, as the image indicates the soft band is dominated by the emission from an extended region, the data were fit with a Raymond & Smith model (1977); this model describes the spectrum of radiation emitted by a hot optically thin plasma with abundances and equilibrium ionization balance appropriate to interstellar conditions. A single-temperature plasma is, again, a poor fit to the data ( $\chi^2/dof = 42.7/18$ ). The possibility of some contribution from the nuclear component was considered. Adding a power-law to the fit yielded a photon index  $\Gamma = 1.73^{+1.14}_{-0.27}$  and  $\chi^2/dof = 19.6/20$ . The absorption to both spectral components was found to be consistent with the Galactic line-of-sight value  $N_H = 1.03 \times 10^{20} \text{ cm}^{-2}$  (Elvis, Lockman & Wilkes 1989). Such a low absorption is consistent with the origin of the soft X-ray emission from regions outside of the nucleus. The nuclear component could be observed as scattered nuclear light, or could represent an unattenuated fraction of the nuclear continuum viewed through holes in the absorber. The parameterization using a Raymond-Smith plasma plus power-law is denoted "Case-1".

Alternatively, the single-temperature plasma may be an inadequate model for the starburst region. A two-temperature solution yielded a significant improvement to the fit with  $\chi^2/dof = 22.6/16$ , a low temperature component  $kT = 0.31^{+0.40}_{-0.03}$  keV, with normalization  $n = 2.3^{+1.3}_{-0.4} \times 10^{-5}$  and hot component  $kT = 1.8^{+60}_{-1.8}$  keV,  $n = 8.3^{+13.2}_{-4.0} \times 10^{-5}$ . The normalization is in units  $10^{-14}/4\pi D^2 \int n_e n_h dV$  where  $D$  is the luminosity distance to the source (cm),  $n_e$  is the electron density ( $\text{cm}^{-3}$ ) and  $n_h$  is the hydrogen density ( $\text{cm}^{-3}$ ). The parameterization using a two-temperature Raymond-Smith plasma is denoted "Case-2".

### 3. The ASCA Observations

The *ASCA* solid-state imaging spectrometers (SISs) and gas imaging spectrometers (GISs) cover the  $\sim 0.4 - 10$  keV and  $\sim 0.8 - 10$  keV bandpasses, respectively. Mrk 231 was observed by *ASCA* 1994 Dec 5. The data were reduced in the same way as the Seyfert galaxies presented in Nandra et al. (1997) and Turner et al. (1997). For details of the data reduction method and instruments see Nandra et al. (1997). Data screening yielded effective exposure times of  $\sim 20$  ks in all four instruments. Examination of the *ASCA* images reveals marginal evidence for F219\_045 in the GIS image, but no evidence for hard X-ray emission from any of the other sources seen in the *ROSAT* images. F219\_015 and F219\_045 are not close enough to be confused with Mrk 231, but there are other sources of contamination as discussed below.

*ASCA* light curves from each instrument were examined over the 0.5-10 keV range, using time bins covering 128s to 5760 s. Mrk 231 was weak and the background light curve showed some low-amplitude variations, however, no flux variations were evident within the *ASCA* observation, which could be attributed to the AGN.

The source flux was  $F \sim (1.0 \pm 0.3) \times 10^{-12} \text{ erg cm}^{-2} \text{ s}^{-1}$  in the 2 – 10 keV band corresponding to an observed luminosity  $L(2 - 10 \text{ keV}) = 8 \times 10^{42} \text{ erg s}^{-1}$ . The soft flux is  $F \sim (1.9 \pm 0.5) \times 10^{-13} \text{ erg cm}^{-2} \text{ s}^{-1}$  in the 0.5 – 2 keV band. This soft flux appears higher than that observed by *ROSAT*, but the *psf* of the *ASCA* instruments is significantly wider than that of the *ROSAT* instruments. This results in some contamination of the soft part of the *ASCA* spectrum by unidentified sources close to Mrk 231, evident in the PSPC and HRI images, as discussed in the following section.

#### 3.1. The ASCA Spectra

*ASCA* SIS data below an energy of 0.60 keV (0.66 keV rest-frame) were excluded from the spectral analysis as it is commonly accepted that there are uncertainties associated with the calibration in that band. The *ASCA* spectra were extracted using circular regions of radii  $3.2'$  and  $6.8'$  for the SIS and GIS instruments, respectively. The PSPC image was then used to examine the sources of contamination in each case. The SIS extraction cell encompasses one source of contamination, and the GIS cell encompasses three. These sources were faint and unidentified, so it is difficult to model the precise contamination from each. However, it was found the contaminating flux from these serendipitous sources could be *parameterized* as 45% (SIS) and 112% (GIS) increases in the normalization of the thermal component ( $kT = 0.31$  keV) used to model the circumnuclear emission in Mrk 231.

### 3.1.1. Case-1

In Case-1 the soft X-ray flux was assumed to originate in a single-temperature Raymond-Smith plasma with some contribution from the nuclear continuum, viewed through unattenuated lines-of-sight or via scattering. The temperature and normalization of the Raymond-Smith plasma were fixed at the values determined from fitting the PSPC data, with an adjustment to account for the soft flux from contaminating sources, as noted above.

The nuclear power-law was modeled assuming attenuation by a column of neutral material,  $N_H$ , at the redshift of the source and with a fraction of the emission assumed to be observed without attenuation. Again, an additional column was fixed at the Galactic line-of-sight value  $N_H = 1.03 \times 10^{20} \text{cm}^{-2}$  (at a redshift of zero). This fit yielded a photon index  $\Gamma \sim 1.9$ , with a column  $N_H \sim 9 \times 10^{22} \text{cm}^{-2}$  covering 79% of the source (fit 1, Table 1).

If the circumnuclear material is ionized, then the column could be higher than that indicated by fits which assume a neutral absorber. The data were fit using models based upon the photoionization code ION (Netzer 1996), once again, an unabsorbed thermal component of fixed temperature and normalization was allowed, the results are shown in Table 1 (fit 2). If the column is assumed to be fully-covering the source, but ionized, then the inferred index is  $\Gamma \sim 1$ . In its simplest interpretation this represents an unusually flat index for the primary continuum. This may indicate another component is present, such as that due to Compton reflection, flattening the observed spectrum. It is not possible to obtain useful constraints on Compton reflection in Mrk 231 (using these data). Therefore the fits were repeated with the photon index fixed at two values often found for Seyfert galaxies (e.g. George et al. 1998 and references therein). This allowed an investigation of the nuclear attenuation under two simple assumptions,  $\Gamma = 1.5$  and  $\Gamma = 2$ . In both these cases, the nuclear absorption was found to be  $\sim 10^{23} \text{cm}^{-2}$  (fits 3-4, Table 1).

A small contribution to iron  $K\alpha$  emission is expected from the thermal component, and is visible in the model plot (Fig 2, top panel). However, no significant line emission was detected from the K-shell of iron, (although a high point on the data/model ratio is duly noted, Fig. 2, bottom panel). These data yield an upper limit (90% confidence) on the equivalent width to be  $EW < 800 \text{ eV}$ . The *ASCA* data do not show a significant line at 0.86 keV, as indicated by the PSPC data, although the spectra are consistent with the presence of a line of the strength inferred by the PSPC data.

### 3.1.2. Case-2

In Case-2 the starburst region was assumed to be parameterized as a two-temperature Raymond-Smith plasma with the temperatures fixed at  $kT = 0.31$  and  $kT = 1.8$  keV, as found in §2. In this case a two-temperature component was allowed in the model, with normalizations fixed at the values derived from the PSPC data (again with an adjustment to the normalization of the cool component to account for flux from the contaminating sources). This parameterization left less soft flux to be attributed to the nucleus and hence inferred different fit parameters to Case-1.

A power-law was considered, attenuated by a column of neutral material at the redshift of the source, again an additional column was fixed at the Galactic line-of-sight value. No unattenuated fraction was allowed. This fit yielded a photon index  $\Gamma \sim 0.6$  (fit 5, Table 1) and the fits were repeated with  $\Gamma = 1.5$  and  $\Gamma = 2$  as before. By fixing the photon index a more meaningful estimate of the column may be obtained,  $N_H \sim 2 - 4 \times 10^{22} \text{cm}^{-2}$  (fits 6 – 7). Fits assuming an ionized absorber yielded column estimates  $N_H \sim 5 \times 10^{22} - 10^{23} \text{cm}^{-2}$ . Whether the absorber is neutral or ionized, Mrk 231 clearly has a hard X-ray continuum component, attenuated by a column consistent with that observed in many Seyfert 2 galaxies (Turner et al. 1997).

## 4. Discussion

The HRI image of Mrk 231 shows emission across several tens of kpc, consistent with the extent of the host galaxy. The soft flux has two peaks of X-ray emission of similar strength in the  $0.1 - 2$  keV band. These peaks are separated by  $\sim 13''$  and the summed emission has  $L(0.5 - 4.5 \text{ keV}) \sim 10^{42} \text{erg s}^{-1}$ , possibly associated with starburst activity in the galaxy. The 60 and  $100 \mu\text{m}$  fluxes can be used to estimate the X-ray luminosity expected from starburst emission in this galaxy, following the prescription of David et al. (1992). Taking the IR fluxes from Smith, Lonsdale and Lonsdale (1998), an associated X-ray luminosity  $L(0.5 - 4.5 \text{ keV}) = 4.43_{-1.86}^{+4.38} \times 10^{42} \text{erg s}^{-1}$  is estimated to originate from a starburst region of the observed IR luminosity. The PSPC flux yields  $L(0.5 - 4.5 \text{ keV}) = 1.43 \pm 0.30 \times 10^{42} \text{erg s}^{-1}$  within an extraction cell of radius  $1.3'$ . The fact the extended X-ray emission yields a lower luminosity than expected either supports the hypothesis that a significant fraction of the IR emission is powered by the active nucleus (Bryant & Scoville 1996) or suggests that the X-ray emission from the starburst is attenuated by material which is more dusty than that observed in the David et al. (1992) sample of galaxies.



Table 1. *ASCA* Spectral Fits

Fit	$\Gamma$	$A^a$	$N_H^b$	$U_X^c/\text{Frac}$	$\chi^2/dof$
Case-1: Neutral Absorber					
1	$1.89^{+1.09}_{-0.56}$	$5.20^{+30.50}_{-5.20}$	$9.1^{+98.9p}_{-9.10}$	$0.79^{+0.17p}_{-0.79p}$	94.0/98
Case 1: Ionized Absorber					
2	$1.10^{+0.78}_{-0.44}$	$1.10^{+2.67}_{-0.48}$	$15.1^{+24.9}_{-15.1}$	$8.91^{+1.09}_{-8.91}$	94.0/98
3	$1.5(f)$	$2.09^{+0.61}_{-0.68}$	$11.7^{+19.8}_{-10.8}$	$2.88^{+5.84}_{-2.88}$	99.2/99
4	$2.0(f)$	$4.42^{+1.50}_{-1.50}$	$11.2^{+9.9}_{-8.0}$	$1.71^{+1.24}_{-1.20}$	104.8/99
Case 2: Neutral Absorber					
5	$0.64^{+0.97}_{-0.48}$	$0.45^{+1.87}_{-0.24}$	$0.2 < 2.7$	...	96.3/99
6	$1.5(f)$	$1.86^{+0.45}_{-0.45}$	$2.1^{+1.7}_{-1.0}$	...	100/100
7	$2.0(f)$	$4.39^{+1.57}_{-1.20}$	$3.7^{+2.7}_{-1.5}$	...	103.6/100
Case 2: Ionized Absorber					
8	$1.03^{+1.50}_{-0.92}$	$0.92^{+9.65}_{-0.73}$	$5.5^{+29.9}_{-5.5}$	$1.22^{+8.78}_{-1.22}$	95.5/98
9	$1.5(f)$	$2.12^{+0.73}_{-0.68}$	$10.5^{+16.5}_{-8.6}$	$1.45^{+2.33}_{-1.45}$	96.1/99
10	$2.0(f)$	$4.69^{+2.05}_{-1.43}$	$12.6^{+15.6}_{-8.4}$	$1.35^{+1.45}_{-1.35}$	98.2/99

<sup>a</sup>The power-law normalization at 1 keV, in units  $10^{-4}$  photons  $\text{s}^{-1}$   $\text{keV}^{-1}$ .

<sup>b</sup>Absorbing column in units  $10^{22}$   $\text{cm}^{-2}$ , at the redshift of the source. An additional column of  $1.03 \times 10^{20} \text{cm}^{-2}$  was included in the fit, at redshift  $z=0$ .

<sup>c</sup>Ionization parameter or covering fraction

$p$  indicates an error estimation hit the limit allowed for that parameter.

An unattenuated thermal component was included in the fits, see text for details

The observed *ASCA* spectrum shows a hard X-ray source exists in Mrk 231. Column measurements range from  $\sim 2 \times 10^{22} - 10^{23} \text{cm}^{-2}$  depending on whether the absorber is assumed to be neutral or ionized, and depending on assumptions about the underlying continuum form. In both cases an unattenuated component was included in the model to describe the extended soft X-ray emission. If the nuclear attenuation is as high as  $N_H \sim 10^{23} \text{cm}^{-2}$  then the intrinsic hard X-ray luminosity is  $L(2 - 10 \text{ keV}) \sim 10^{43} \text{erg s}^{-1}$ . Extrapolation of the *ASCA* fits to the 50 – 200 keV band yield an estimated  $\gamma$ -ray luminosity  $L(50 - 200 \text{ keV}) \sim 10^{43} \text{erg s}^{-1}$ , significantly lower than the OSSE upper limit of  $L(50 - 200 \text{ keV}) < 2 \times 10^{45} \text{erg s}^{-1}$  (Dermer et al. 1997; assuming our value for  $H_o$ ).

The column density derived from fits which assume a neutral absorber are in approximate consistency with the value of  $10^{22} \text{cm}^{-2}$  estimated from the BAL absorbing systems (Rudy, Foltz and Stocke 1985) perhaps indicating an association with that gas. The presence of the  $10 \mu m$  silicate absorption feature and the relative levels of Na and Ca features (Rudy et al. 1985) along with the high polarization (Smith et al. 1995) show that there is a great deal of circumnuclear dust. Furthermore, Weymann et al. (1991) note that BAL clouds with high enough column density to produce the FeII and FeIII absorption (as seen in Mrk 231) are consistent with the existence of dust within the clouds. C and O may be incorporated into molecules in such dusty material, and consequently depleted in the gas-phase compared to the levels assumed in models used here for the X-ray absorption, this may result in X-ray column measurements which underestimate the nuclear absorption by a factor of  $\sim$  several.

#### 4.1. Is Mrk 231 X-ray quiet?

It is interesting to investigate whether these new measurements of the nuclear absorption suggest Mrk 231 is intrinsically X-ray quiet, or whether the X-ray attenuation can account for its appearance as such. Green et al. (1995) found BAL QSOs to be X-ray weak using observed *ROSAT* PSPC fluxes; i.e. 30 – 100 times less luminous in the 0.1 – 2 keV band than would be expected by extrapolation from their optical luminosities. The PSPC spectra did not allow Green et al. (1995) to determine whether this X-ray weakness was due to absorption of the X-rays by a large column of material, or whether the sources were intrinsically weak. An *ASCA* observation of PHL 5200 (Mathur, Elvis and Singh 1995) had low signal-to-noise but indicated the presence of an absorbing column  $N_H \sim 10^{23} \text{cm}^{-2}$  attenuating the nuclear X-rays.

Lawrence et al. (1997) compiled flux and line measurements across the broad-band spectrum for a sample of AGN with strong FeII emission, and examined correlations between

the various quantities. Those authors used the *ROSAT* PSPC data from Mrk 231 and derived indices  $\alpha_{ix} = 1.97$  and  $\alpha_{ox} = 1.76$  between the  $1\mu m$  and 2 keV flux, and between the 2500Å and 2 keV flux, respectively. Mrk 231 was found to be a persistent outlier on their correlation plots, often due to the weakness in the X-ray band. Furthermore, Lawrence et al. (1997) found the *ROSAT* PSPC spectrum to rule out the presence of a large column density ( $N_H \gtrsim 10^{21}\text{cm}^{-2}$ ) for the X-ray absorber, producing a spectral paradox because a large column is required to bring the spectral-energy-distribution into line with other strong FeII emitters. However, as previously discussed, the PSPC spectrum is complex and contains a significant contamination from a region of extended emission, which has a lower absorption than the nucleus. The PSPC is also insensitive to column densities  $> 10^{22}\text{cm}^{-2}$ . The *ASCA* data allow a more accurate determination of large absorbing columns and hence a more accurate determination of the intrinsic 2 keV flux from the nucleus. Combining this information with the *ROSAT* results we can subtract off the contamination and obtain a more accurate estimate of the nuclear flux at 2 keV. Thus the energy indices were recalculated using the *ASCA* measurement of the intrinsic nuclear flux at 2 keV; an absorption correction was applied and the estimated contribution to X-ray flux from the region of extended emission was subtracted.

Smith et al. (1995) show a Faint Object Spectrograph (FOS) spectrum which has an observed flux  $\sim 2 \times 10^{-27}\text{erg cm}^{-2} \text{ s}^{-1} \text{ Hz}^{-1}$  at a rest-energy of 2500Å. It is difficult to estimate the reddening-correction which should be applied to this 2500Å flux; dust is thought to be an important constituent of the circumnuclear material, but there is no 2200Å dust feature in the FOS spectrum (Smith et al. 1995). Laor and Draine (1993) show absorption cross-sections per H nucleus calculated assuming a range of differing dust grain types and size distributions. I assume a cross-section in the middle of their range of models, i.e.  $\tau \sim 10^{-22}N_H^{-1}\text{cm}^2$ . If the lowest realistic value of X-ray absorption is taken,  $N_H = 2 \times 10^{22}\text{cm}^2$  (Table 1), then a corrected 2500Å flux  $\sim 1.5 \times 10^{-26}\text{erg cm}^{-2} \text{ s}^{-1} \text{ Hz}^{-1}$  is obtained. If  $N_H \sim 10^{23}\text{cm}^{-2}$  then the reddening-corrected flux is  $\sim 4.6 \times 10^{-23}\text{erg cm}^{-2} \text{ s}^{-1} \text{ Hz}^{-1}$  at 2500Å.

In Case-1, the *ASCA* data imply an intrinsic (absorption-corrected) nuclear flux of  $1.7 \times 10^{-30}\text{erg cm}^{-2} \text{ s}^{-1} \text{ Hz}^{-1}$  at 2 keV, assuming a power-law partially covered by neutral material (the first fit in Table 1), after subtracting the contamination from sources evident in the *ROSAT* data. Considering the range of possible values for absorption-corrected optical flux yields  $1.51 < \alpha_{ox} < 2.85$ . In Case-2, the inferred 2 keV flux from the nucleus is  $8.2 \times 10^{-31}\text{erg cm}^{-2} \text{ s}^{-1} \text{ Hz}^{-1}$  at 2 keV, assuming the absorber is neutral material, and  $\Gamma = 1.5$  (fit 6 in Table 1). This case yields  $1.64 < \alpha_{ox} < 2.97$ . Assumption of an ionized absorber in Case-2, with  $\Gamma = 1.5$  (fit 9, Table 1),  $N_H \sim 10^{23}$  yields a 2 keV flux  $\sim 9.3 \times 10^{-31}\text{erg cm}^{-2} \text{ s}^{-1} \text{ Hz}^{-1}$  at 2 keV and  $1.62 < \alpha_{ox} < 2.95$ . Estimating the  $1\mu m$  flux

from Rigopoulou et al. (1996) yields  $\alpha_{ix} \sim 1.7 - 1.8$  for Case-1 and Case-2, respectively.

These new indices do not bring Mrk 231 into the distribution of properties seen for other strong FeII emitters (Lawrence et al. 1997). Furthermore, the lower limit in Case-1 lies just above the range  $\alpha_{ox} \sim 1.1 - 1.5$  found for Seyfert 1 galaxies (Kriss & Canizares 1985). However, all estimates of  $\alpha_{ox}$  are consistent with the range  $\alpha_{ox} \sim 1.3 - 1.9$  observed for the radio-quiet quasars, ie. the higher luminosity sources studied by Kriss & Canizares (1985). As a Seyfert galaxy it would be considered to be at the X-ray-weak end of the distribution of indices for that class, but amongst QSOs it would not be considered X-ray-weak at all. The nominal ranges for  $\alpha_{ox}$  combined with the absence of narrow emission lines in the optical bandpass, the presence of BAL systems and the high bolometric luminosity of Mrk 231 suggests the source is closer in nature to a QSO than a Seyfert galaxy.

## 5. Summary

An HRI image of Mrk 231 shows extended emission in the 0.1 – 2 keV band, of size-scale  $\sim 30$  kpc in diameter, cospatial with the host galaxy. The nucleus itself appears faint in the soft X-ray band, probably due to absorption. The extended emission has a luminosity  $L(0.1 - 2 \text{ keV}) \sim 10^{42} \text{ erg s}^{-1}$  and is probably associated with starburst activity in the galaxy. The relative levels of IR and X-ray emission suggest some of the IR emission has an origin other than starbursts, or that the starburst region has a higher dust content than observed in other starburst galaxies.

An *ASCA* observation revealed a hard X-ray source in Mrk 231. The spectrum indicates the X-ray column density is  $N_H \sim 2 \times 10^{22} - 10^{23} \text{ cm}^{-2}$ , attenuating the nuclear X-rays. Consideration of the appropriate absorption-corrections to the optical and X-ray data infer an underlying spectral-energy-distribution for Mrk 231 which is more like that of a QSO than a Seyfert 1 galaxy.

## 6. Acknowledgements

I am grateful to *ASCA* team for their operation of the satellite and to Ian George and Richard Mushotzky for useful comments. Thanks to Keith Mason for confirmation of the optical positions of some AGN in the *ROSAT* field-of-view, and to Hagai Netzer for use of tables based upon ION. This research has made use of the NASA/IPAC Extragalactic database, which is operated by the Jet Propulsion Laboratory, Caltech, under contract with NASA; of the Simbad database, operated at CDS, Strasbourg, France; and data obtained

through the HEASARC on-line service, provided by NASA/GSFC. I acknowledge the financial support of the Universities Space Research Association, University of Maryland, Baltimore County and LTSA grant NAG5-7385.

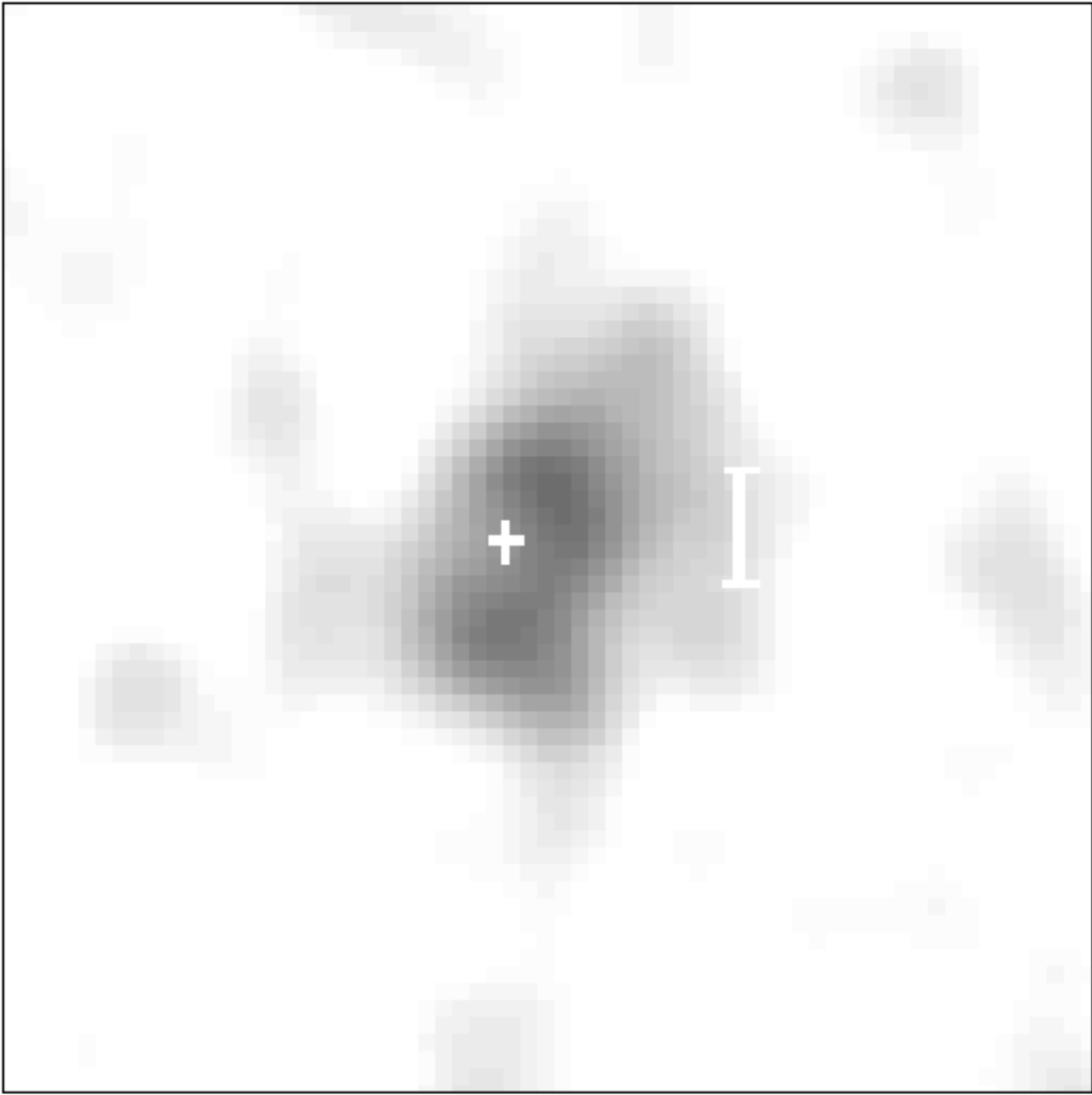


Fig. 1.— The *ROSAT* HRI image of Mrk 231, in  $1''$  pixels smoothed with a gaussian function with  $\sigma = 1.5''$ . The orientation is such that North is at the top of the image, and East is to the left. The position of the radio nucleus is marked with a white cross, the bar represents  $10''$  which is equal to  $\sim 10$  kpc at the redshift of the source.

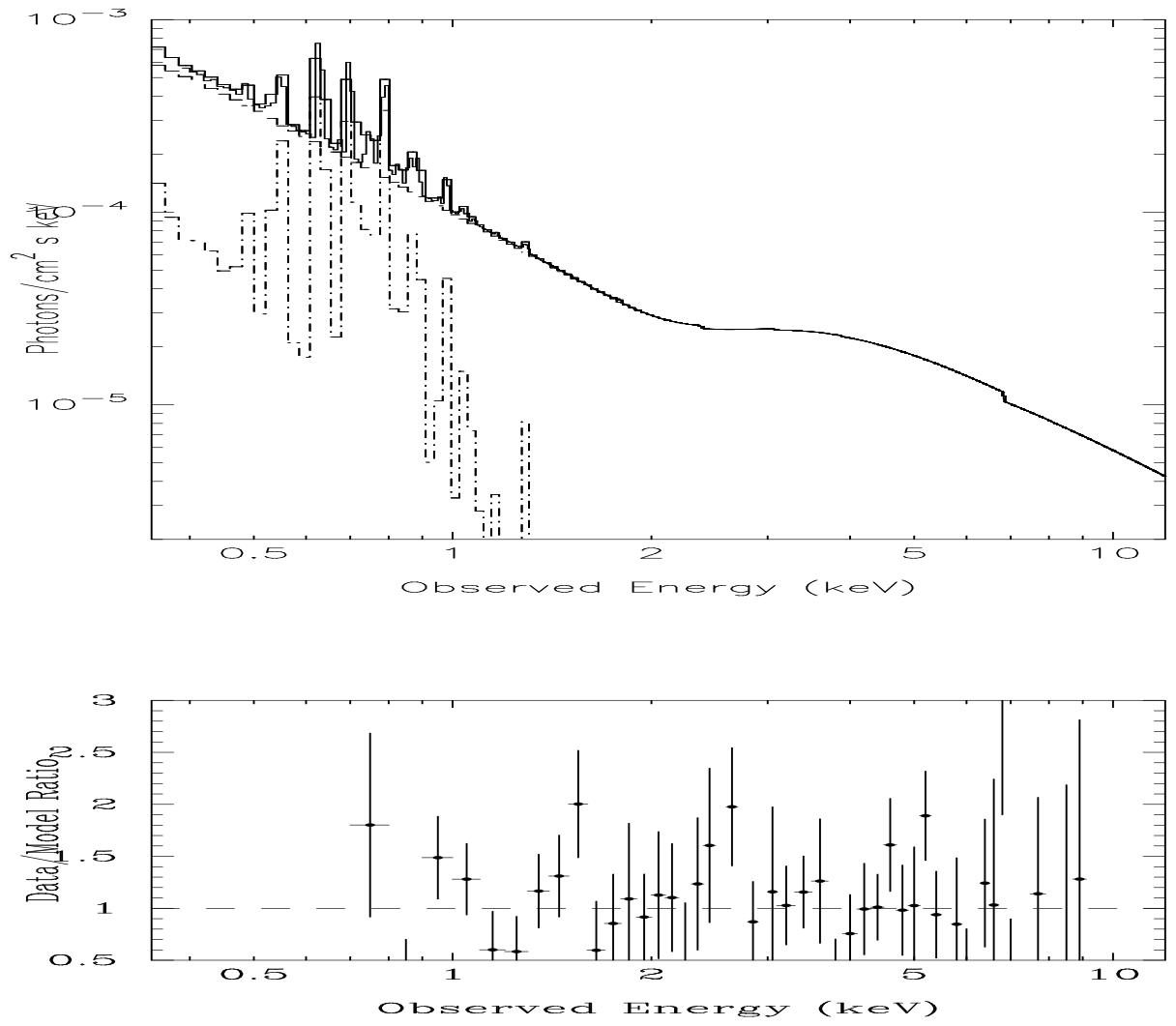


Fig. 2.— *Top Panel:* The unfolded spectrum, from a fit to a power-law attenuated by an absorber partially covering the source (fit 1, see Table 1). *Bottom Panel:* The data/model ratio for the *ASCA* instruments, versus the power-law model with index left free and a neutral absorber partially covering the source

## REFERENCES

- Adams, T.F. 1972, ApJ, 176, L1
- Arakelian, M.A., Dibai, E., Esipov, V., Markarian, B. 1971, Astrofizika, 7, 177
- Baan, W.A. 1985, Nature, 315, 26
- Boksenberg, A., Carswell, R.F., Allen, D.A., Fosbury, R.A.E., Penston, M.V., Sargent, W.L.W. 1977, ApJ, 178, 451
- Boroson, T.A., Meyers, K.A., Morris, S.L., Persson, S.E. 1991, ApJ, 370, L19
- Brain, J., Dumke, M. 1998, A&A, 333, 38
- Bryant, P.M., Scoville, N.Z. 1996, ApJ, 457, 678
- David, L. P., Jones, C., Forman, W. 1992, ApJ, 388, 82
- Dermer, C.D., Bland-Hawthorn, J.B., Chiang, J., McNaron-Brown, K. 1997, ApJ, 484, L121
- Elvis, M., Lockman, F.J., Wilkes, B.J. 1989, AJ, 97, 3
- Forster, K., Rich, R.M., McCarthy, J.K. 1995, ApJ, 450, 74
- George, I.M., Turner, T.J., Netzer, H., Nandra, K., Mushotzky, R.F., Yaqoob, Y. 1998, ApJS, 114, 73
- Green, P. et al. 1995, ApJ, 450, 51
- Hartig, G.F., Baldwin, J.A. 1986, ApJ, 302, 64
- Kollatschny, W., Dietrich, M., Hagan, H. 1992, ApJ, 264, L5
- Kriss, G.A., Canizares, C.R. 1985, ApJ, 297, 177
- Laor, A., Draine, B.T. 1995, ApJ, 402, 441
- Lawrence, A., Elvis, M., Wilkes, B.J., McHardy, I., Brandt, N. 1997, MNRAS, 285, 879
- Lipari, S., Colina, L., Macchetto, F. 1994, ApJ, 427, 174
- Lipari, S., Terlevich, R., Macchetto, F. 1993, ApJ, 406, 451
- Mathur, S., Elvis, M., Singh, K.P. 1995, ApJ, 455, L9
- Nandra, K., George, I.M., Mushotzky, R.F., Turner, T.J., Yaqoob, T. 1997, ApJ, 476, 70
- Raymond, J.C., Smith, B.W. 1977, ApJS, 35, 419
- Reicke, G.H., Low, F.J. 1972, ApJ, 176, L95
- Rigopoulou, D.A., Lawrence, A., Rowan-Robinson, M. 1996, MNRAS, 278, 1049
- Roche, P.F., Aitken, D.K., Whitmore, B. 1983, MNRAS, 205, 21



- Rudy, R.J., Foltz, C.B., Stocke, J.T. 1985, ApJ, 288, 531
- Sanders, D.B., Soifer, B.T., Elias, J.H., Madore, B.F., Matthews, K., Neugebauer, G.,  
Scoville, N.Z. 1988, ApJ, 325, 74
- Scoville, N. Z., Sanders, D.B., Sargent, A.I., Soifer, B.T., Tinney, C.G. 1989, ApJ, 345, L25
- Smith, H.E., Lonsdale, Colin J., Lonsdale, Carol, J. 1998, ApJ, 492, 137
- Smith, P.S., Schmidt, G.D., Allen, R.G., Angel, J.R.P. 1995, ApJ, 444, 146
- Soifer, B.T., Sanders, D., Madore, B.F., Neugebauer, G., Danielson, G.E., Elias, J.H.,  
Lonsdale, C.J., Rice, W. 1987, ApJ, 320, 238
- Soifer, B.T., Sanders, D., Madore, B.F., Neugebauer, G., Danielson, G.E., Lonsdale, C.J.,  
Persson, S.E. 1986, ApJ, 303, L41
- Surace, J., Sanders, D.B., Vacca, W.D., Veilleux, S., Mazzarella, J.M. 1998, ApJ, 492, 116
- Turner, T.J., George, I.M., Nandra, K. & Mushotzky, R.M. 1997, ApJS, 113, 23
- Voit, G.M., Weymann, R.J., Korista, K.T. 1993, ApJS, 88, 357
- Weymann, R.J., Morris, S.L., Foltz, C.B., Hewett, P.C. 1991, AJ, 373, 23
- Xia, X.-Y., Boller, Th., Wu, H., Deng, Z.G., Gao, Y., Zou, Z.L., Mao, S., Boerner, G. 1998,  
ApJ, 496, L9